

## **Theory of Irreversible Processes in Nonequilibrium Quantum Systems. II. Cluster Expansions with Contraction for Homogenous Systems**

**Tomio Yamakoshi Petrosky<sup>1</sup>**

*Received January 11, 1979*

---

On the basis of a method developed in a previous paper, a systematic rule for obtaining a symmetrized collision superoperator of the Van Hove generalized master equation including an arbitrary number of particles is given. In the formalism, the quantum statistical effect is taken into account through the use of contractions (internal and external contractions) on the basis of the cluster expansion. As an application of this general rule, a symmetrized collision superoperator including the effect of three-particle collisions is obtained.

---

**KEY WORDS:** Many-particle collision superoperator; cluster expansion; internal and external contractions.

### **1. INTRODUCTION**

This second paper in the present series investigates the effects of multiple collisions in the generalized master equation on the basis of a new treatment of the quantum statistical effect through the use of contractions, using a diagrammatic method given previously<sup>(1)</sup> (this work will be cited as I). In I, we derived a kinetic equation for a weakly coupled system based on the expansion of the collision superoperator (s.operator) in powers of the coupling constant  $\lambda$ . However, for the case of a strong interaction, divergences appear in the  $\lambda$  expansion and partial summations of infinite series must be performed to get an expansion in terms of a bounded operator of the binary cluster. This problem has been investigated by Résibois<sup>(2)</sup> and also by Swenson.<sup>(3)</sup> They derived kinetic equations including the effect of three-particle collisions for a simple unsymmetrized quantum system. However,

---

<sup>1</sup> Department of Physics, Science University of Tokyo, Kagurazaka, Shinjuku-ku, Tokyo, Japan.

due to the complicated structure of the quantum statistical effects in multiple collisions, no symmetrized effects were investigated except for the simplest case of the two-particle collision by Prigogine and Résibois.<sup>(4)</sup>

The aim of the present work is to show how our new treatment for the quantum statistical effect in I can be used to deal with such complicated effects in multiple collisions. With the aid of our diagrammatic method with the use of contractions we can separate the quantum statistical effects in multiple collisions into an external effect and an internal one. The external effect is a degenerating effect between a particle in a collision and a particle in the background of this collision, and is indicated by an external contraction in our diagrams. The internal effect is a degenerating effect among the particles in a collision and is indicated by an internal contraction in our diagrams. By virtue of this classification, it becomes possible to separate the quantum statistical effects in the essentially multiple collision from the so-called Uehling-Uhlenbeck term arising from the statistical effects of the background particles. Then, on the basis of this classification and using the cluster expansion, we obtain a systematic rule for obtaining the symmetrized collision s.operator including an arbitrary number of particles.

In the next section, starting with the construction of unsymmetrized collision s.operators based on the cluster expansion, we give a systematic rule for obtaining a symmetrized collision s.operator including an arbitrary number of particles. Section 3 is devoted to applications of our general rule and there the symmetrized collision s.operators including the effects of two- and three-particle collisions are obtained. By using these s.operators, we further derive a kinetic equation of a momentum distribution function under the condition of an instantaneous collision. In the last section, some implications of our results are discussed.

## 2. CONSTRUCTION OF COLLISION S.OPERATOR

The collision s.operator  $\chi_E(l)$  in which we are interested appears in the generalized master equation

$$i\hbar \partial_t \rho_{0,E}(|\mathbf{p}^N; t\rangle) = h_E(\mathbf{p}^N; t) + \frac{2\pi}{\hbar} \int_0^t d\tau \sum_{\mathbf{p}'^N} (\mathbf{p}^N; \mathbf{p}^N | \chi_E'(\tau) | \mathbf{p}'^N; \mathbf{p}'^N) \rho_{0,E}(|\mathbf{p}'^N; t - \tau\rangle) \quad (2.1)$$

where

$$(\mathbf{p}^N; \mathbf{p}^N | \chi_E'(t) | \mathbf{p}'^N; \mathbf{p}'^N) = \left( \frac{1}{2\pi i} \right)^2 \int_{\gamma} dl e^{-itl/\hbar} (\mathbf{p}^N; \mathbf{p}^N | \chi_E(l) | \mathbf{p}'^N; \mathbf{p}'^N) \quad (2.2)$$

The partial distribution function of momenta  $\rho_{0,E}(|\mathbf{p}^N; t)$  is related to the vacuum component of the Wigner distribution function  $\rho_0(\mathbf{p}^N; t)$  for  $t > 0$  as

$$\rho_0(|\mathbf{p}^N; t) = \int_{-\infty}^{+\infty} dE \rho_{0,E}(|\mathbf{p}^N; t) \quad (2.3)$$

In (2.1), the same notations are used as in Ref. 1, Section 3, for the inhomogeneous term  $h_E$  and for the collision s.operator  $\chi_E$ , including the quantum statistical effect through the use of contractions. The diagrams corresponding to the collision s.operator are shown in Fig. 1, where the first part of the right side is the gain part of the collision s.operator and the second part is the loss part.

We now give a rule for constructing the quantum statistical collision s.operator based on the cluster expansion of the diagonal fragments  $\mathcal{W}$  and  $G$ . Our construction is achieved by using the diagrammatic method as follows: (i) First, we construct the unsymmetrized one-sided diagonal fragment on the basis of the cluster expansion. (ii) Next, by symmetrizing the fragments through a contraction, we find the quantum statistical skeleton fragments. (iii) Then, with the aid of the compensative relation, we find two-sided skeleton fragments. (iv) Finally, by putting external degenerating contractions, and by piling up one-sided diagonal fragments on the above skeleton fragments as bubbles, and furthermore by attaching inactivated diagonal fragments to the two-sided fragment, we obtain the collision s.operator.

Let us now explain each step in this procedure in detail.

(i) To construct the unsymmetrized one-sided fragment, we first introduce a diagrammatic notation for the "one-sided  $n$ -particle cluster." This is defined by the summation of all diagrams that include  $n$  colliding particles connected through their interactions and having no intermediate states equal to the initial and final states. Examples of clusters are shown in Fig. 2.

In each cluster, diagrams are classified into two groups, "irreducible clusters" and "reducible clusters." The irreducible cluster is defined by the summation of all diagrams including neither "bubbles" nor "semibubbles" in the intermediate state. Here, a semibubble is a part of a diagram corresponding to a transition between states of the same momentum, but in which only the roles of two particles are interchanged. An example of a semibubble is shown in Fig. 3a. We need to separate such a semibubble from other transitions, because it may reduce to the quantum statistical bubble through a contraction. For example, by the contraction between particles 2 and 3 in Fig. 3a, the semibubble reduces to a bubble as in Fig. 3b. In Fig. 4, some examples of irreducible clusters are shown.

The reducible clusters are defined by the remaining parts of clusters and

$$\chi_E = \sum_{i=0}^{\infty} \left( (\overset{\cdot}{G})^{*i} + (\overset{\cdot}{G})^{*i} \right) * \left( \overset{\cdot}{W} + ((\overset{\cdot}{G}) + (\overset{\cdot}{G})) \right)$$

Fig. 1. Diagrams corresponding to the collision s. operator.

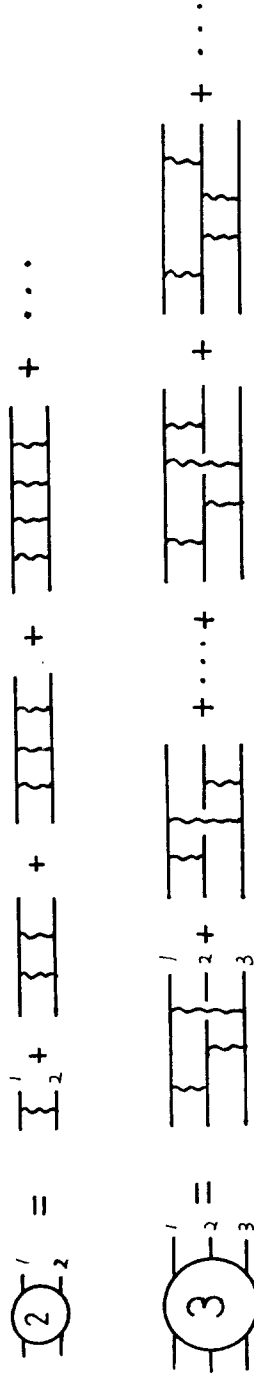


Fig. 2. Examples of clusters.

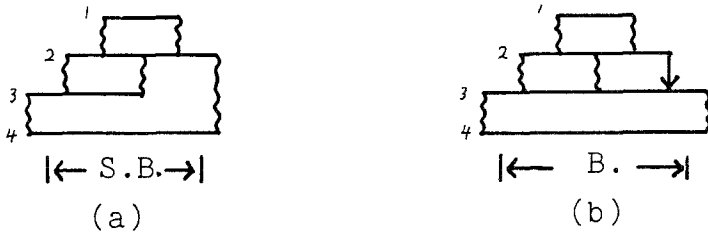


Fig. 3. (a) Semibubble (S.B.); (b) Bubble (B.).

are always constructed by combining irreducible clusters. The three-particle cluster, for example, is constructed from irreducible clusters as shown in Fig. 5.

Independent of the above classification, we need to further classify the clusters into two groups: (1) Clusters that yield an external contraction by symmetrization through a contraction, and are called the “concave type of cluster” or the “concave cluster” according to its topological structure. A typical diagram in the concave cluster is shown in Fig. 6a, where, by contraction between 1 and 2, an external contraction is yielded as in Fig. 6b. (2) Clusters that yield no external contraction, and are called the “convex type of cluster” or the “convex cluster.” An example of this type is shown in Fig. 6c.

By performing contractions in the above-classified clusters, the symmetrization of the one-sided diagonal fragments is achieved.

(ii) We now give a rule for finding a quantum statistical skeleton fragment by performing a contraction on an unsymmetrized cluster. The simplest symmetrized skeleton fragment is obtained from a convex type of irreducible cluster. Indeed, on the performance of a contraction in this cluster, there appears neither an external contraction nor a bubble. For example, the symmetrization of the three-particle irreducible cluster through all possible contractions gives the quantum statistical skeleton fragments shown in Fig. 7, where the symmetrization operator defined in (2.10) of I is used to represent the summation of the contracting arrows in compact form.

The symmetrization of a concave cluster is more complicated, since some of the contractions yield external contractions. To get a skeleton fragment without an external contraction, we must subtract the part of the symmetrization that yields the external contraction from a simple symmetrization among all particles appearing in the cluster. This subtraction is not so difficult, because if the external contraction is removed after performing this contraction, the cluster becomes simpler than the original one. Then, from this simpler cluster, we can find which part of the symmetrization must be

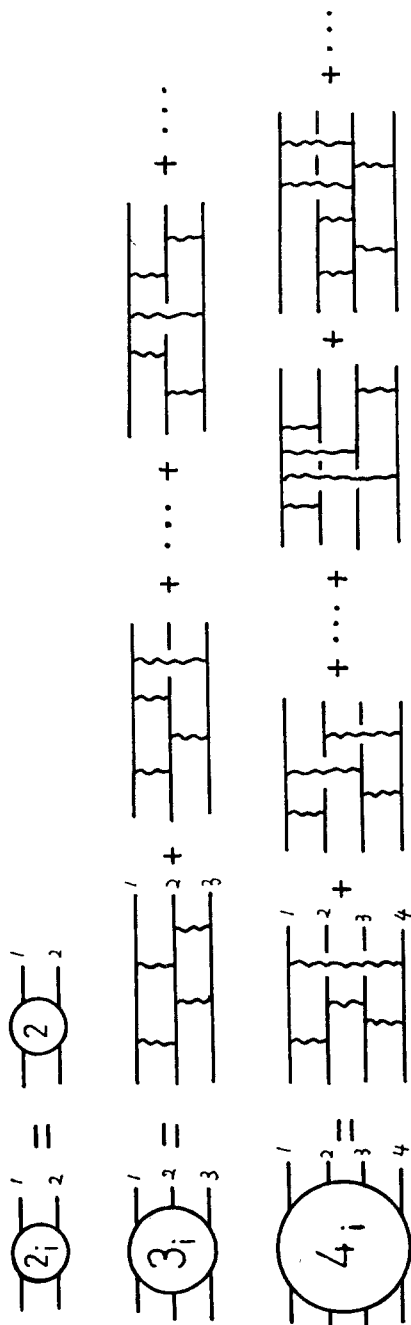


Fig. 4. Examples of irreducible clusters.

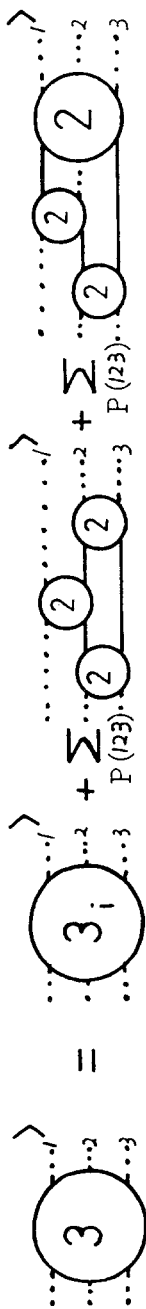


Fig. 5. Three-particle one-sided fragment expressed by irreducible clusters, where the summation runs over all permutations of particles 1, 2, and 3.

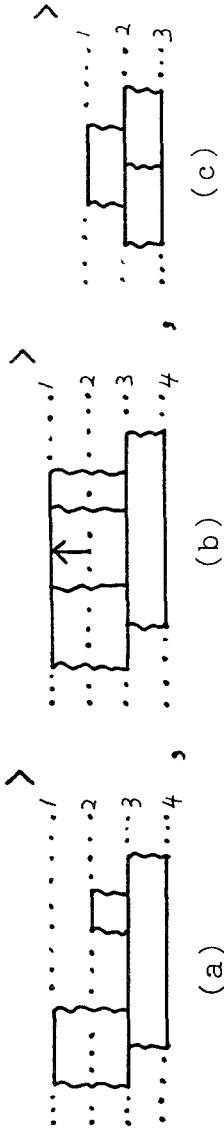


Fig. 6. (a) Typical diagram in a concave cluster. (b) External contraction obtained from a symmetrization of the concave cluster (a). (c) Typical diagram in a convex cluster.

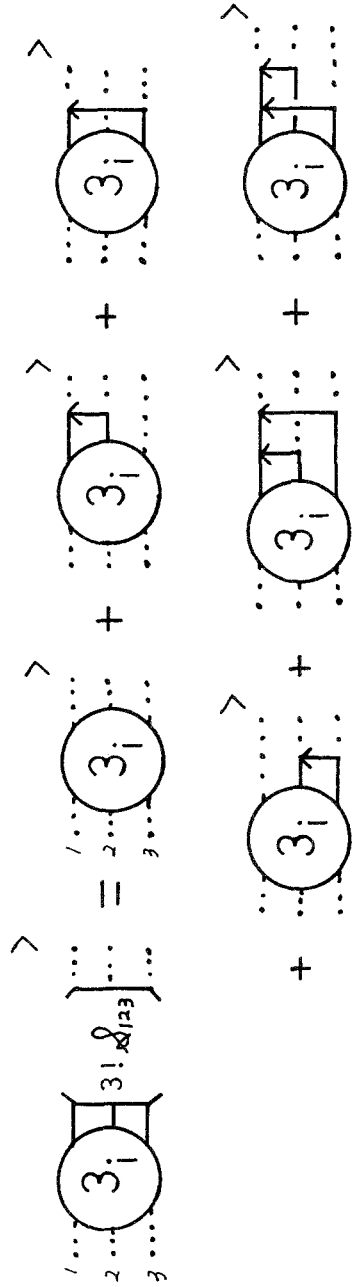


Fig. 7. Symmetrization of a three-particle irreducible cluster through all possible contractions.

subtracted. For example, in Fig. 8a the contraction between particles 1 and 2 in the concave diagram is the external contraction shown in Fig. 8b.<sup>2</sup> By removing this contracting arrow, the diagram becomes a simpler convex type of three-particle irreducible cluster. Thus, the diagram in Fig. 8b can be safely symmetrized without further external contraction as in Fig. 8d. There,  $Q_{ij}$  is the interchanging operator introduced in Section 2 of I. Then, by subtracting the partially symmetrized cluster from the simple symmetrized cluster among all particles 1–4, we obtain the quantum skeleton fragment in Fig. 8e.

More complicated concave clusters can be symmetrized by iterative use of the subtracting procedure for partially symmetrized clusters similar to this simple example. An example of a quantum statistical skeleton fragment obtained from a more complicated concave cluster is shown in Fig. 9, where the terms from second to fourth are symmetrized clusters with single external contraction and the last term is with two external contractions.

Next, we consider the symmetrization of a reducible cluster. It should be noted that in the symmetrization of a cluster having a bubble, there are some contractions that cause the bubble to reduce to a nonbubble such as in Fig. 10a. Therefore, in constructing the quantum statistical skeleton fragment, we cannot omit the reducible cluster from our consideration, even if it has a bubble in the unsymmetrized cluster. For such a case, the quantum statistical skeleton fragment can be found by subtracting the quantum statistical cluster with a bubble from the simple symmetrized one among all particles appearing in the cluster. Therefore, we must first find the part of the symmetrization that yields a quantum statistical cluster with a bubble. As can be seen in the example of Fig. 10b, such a symmetrization is attained if the symmetrization of the basic skeleton fragment is combined with the partial symmetrization of the bubble except for the particle connecting to the basic skeleton fragment. The diagram in Fig. 10c is thus the quantum statistical skeleton fragment for which we are looking.

The more complicated quantum statistical skeleton fragment originating from the unsymmetrized cluster having more than a single bubble can be found by iterative use of the subtracting procedure of quantum statistical clusters with bubbles similar to this simple example. An example is shown in Fig. 11, where the first parenthesis indicates the symmetrization without the external contraction, the second and the third parentheses indicate the symmetrization with a single bubble, and the last term indicates the symmetrization with two bubbles.

For the case of the symmetrization of a reducible cluster with a semi-

<sup>2</sup> In order to avoid ambiguity in the location of the potential lines between particles 3 and 4 in each cluster in Fig. 8, we take it that the right cluster in each diagram does not contain the potential lines between these particles at its leftmost side.



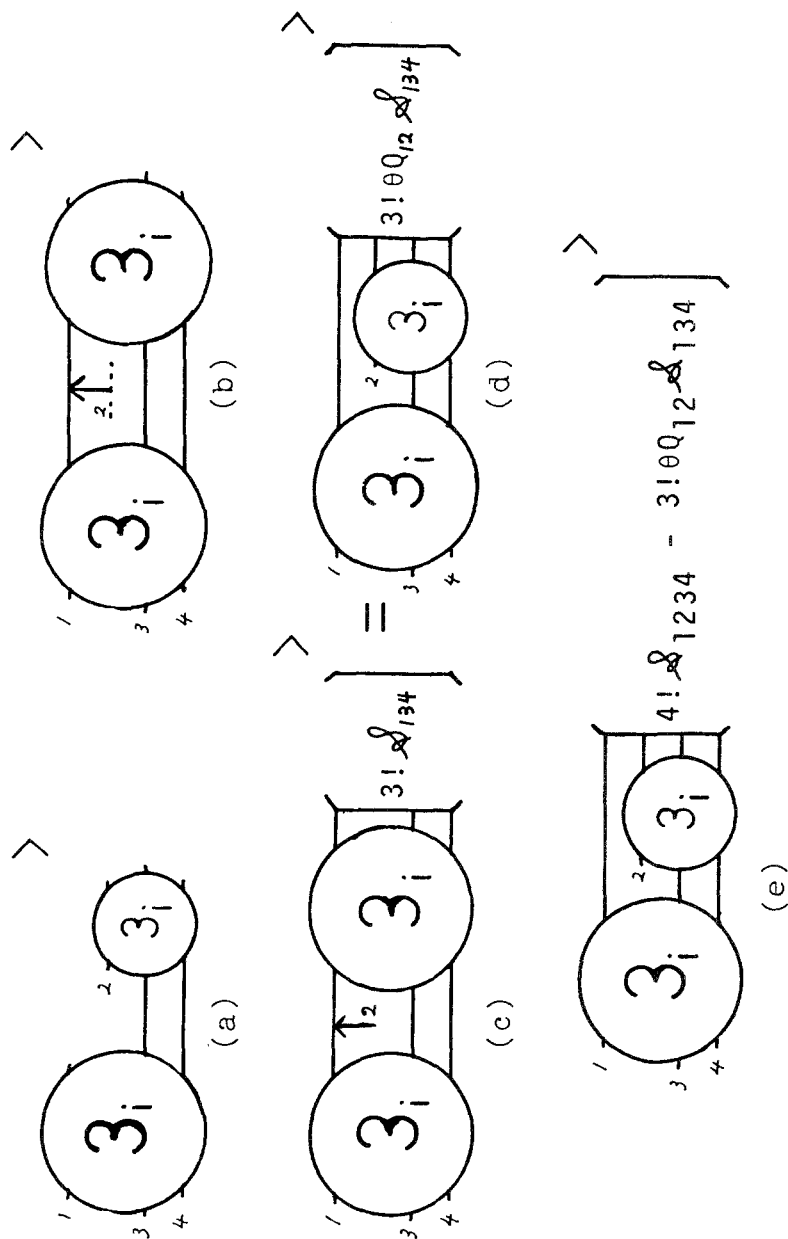


Fig. 8. Symmetrization of a concave cluster.



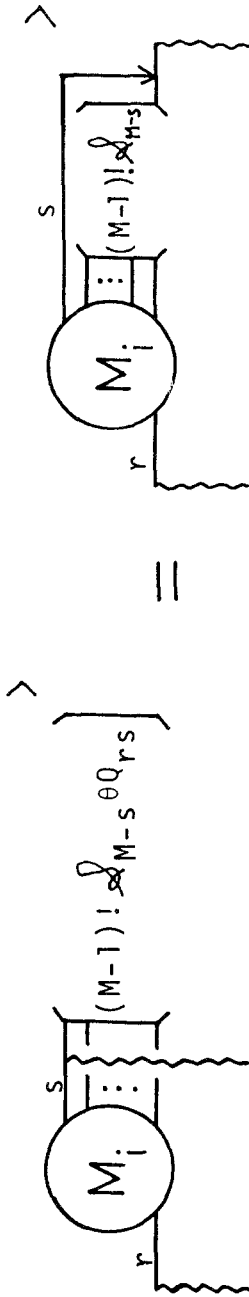


Fig. 12. Symmetrization which causes a semibubble to be reduced to a quantum statistical bubble.

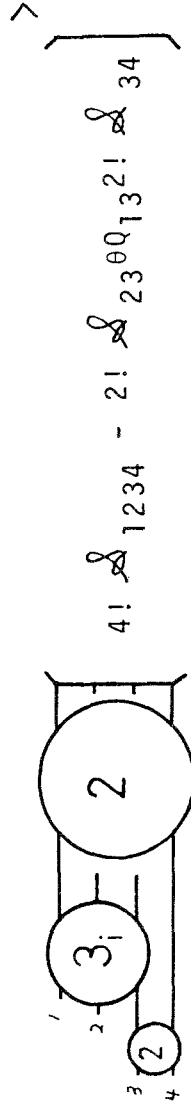


Fig. 13. Example of a quantum statistical skeleton fragment obtained from a reducible cluster having a semibubble.

bubble, it is enough to notice that only a part of the symmetrization in Fig. 12 causes the semibubble to reduce to the quantum statistical bubble. There, the subscript  $M - s$  on  $\mathcal{S}$  means the set of particles constructing the semibubble except for particle  $s$ . If in the above rule for the symmetrization for a cluster with bubbles we replace the partial symmetrization of the bubble with the symmetrization in Fig. 12, we get the rule for obtaining a quantum statistical skeleton fragment from a cluster with semibubbles. For example, corresponding to Fig. 10c, we get the quantum statistical skeleton fragment as shown in Fig. 13, where  $2! \mathcal{S}_{23} \theta Q_{13}$  appears instead of  $2! \mathcal{S}_{12}$  in Fig. 10c.

As a consequence of the above procedures (i)–(iv), the quantum statistical collision s.operator of the generalized master equation (2.1) can be obtained.

### 3. APPLICATIONS

We now apply our analysis to the derivation of the kinetic equation for the one-particle momentum distribution function for a simple system in which two- and three-particle collisions cannot be neglected. The general equation can be obtained from the reduction of (2.1) as

$$\begin{aligned}
 & i\hbar \partial_t \phi_{1,E}(\mathbf{p}_1, t) \\
 &= \sum_{r=2} h_E^{(r)}(\mathbf{p}^r; t) + \frac{2\pi}{\hbar} \int_0^t d\tau \sum_{r=2} (h^3 c)^{r-1} \\
 & \quad \times \sum_{\mathbf{p}^{r-1}} \sum_{\mathbf{p}^{r'}} \langle \mathbf{p}^r; \mathbf{p}^r | \chi_E^{(r)}(\tau) | \mathbf{p}^{r'}; \mathbf{p}^{r'} \rangle \prod_{i=0}^{r-1} \phi_{1,E}(\mathbf{p}_i, t - \tau) \quad (3.1)
 \end{aligned}$$

with

$$\phi_1(\mathbf{p}_i, t) = \int_{-\infty}^{+\infty} dE \phi_{1,E}(\mathbf{p}_i, t) \quad (3.2)$$

Here the reduction  $(\hbar^3 \Omega^{-1})^{N-1} \sum_{\mathbf{p}^{N-1}}$  except for the fixed particle 1 has been performed, and the  $(r)$  on  $h_E$  and  $\chi_E'$  means that the quantities are related to  $r$  particles;  $c$  is the concentration of the system.

Let us first consider the simplest case, corresponding to two-particle collision. The quantum statistical one-sided skeleton fragment for this case is shown in Fig. 14. From this diagram, we can easily obtain the two-sided diagonal fragment by using the compensative relation. Then, the two-particle collision s.operator is as given by Fig. 15. In this simplest case, neither

external contractions nor bubbles and inactivated one-sided diagonal fragments appear. The right side in Fig. 15 can be expressed in terms of the two-particle  $T$ -matrix defined by the equation

$$T_{12}(E, I) = V_{12} - V_{12} \frac{1}{H_{12}^0 - E - (I/2)} T_{12}(E, I) \quad (3.3)$$

where  $H_{12}^0$  is the unperturbed two-particle Hamiltonian and

$$\langle \mathbf{p}_i, \mathbf{p}_j | V_{i,j} | \mathbf{p}'_i, \mathbf{p}'_j \rangle = \Omega^{-1} \sum_{\mathbf{q}} \lambda v(q) \delta^{\mathbf{K}}(\mathbf{p}_i - \mathbf{p}'_i + \hbar \mathbf{q}) \delta^{\mathbf{K}}(\mathbf{p}_j - \mathbf{p}'_j - \hbar \mathbf{q}) \quad (3.4)$$

Then, the gain part of the two-particle  $s$ -operator is

$$\begin{aligned} & (\mathbf{p}^2; \mathbf{p}^2 | \Delta_E^{(0)}(I) \mathcal{W}_E^{(2)}(I) | \mathbf{p}'^2; \mathbf{p}'^2) \\ &= 2! \left( \frac{1}{E_{\mathbf{p}^2} - E - (I/2)} - \frac{1}{E_{\mathbf{p}^2} - E + (I/2)} \right) \\ & \quad \times \langle \mathbf{p}_1, \mathbf{p}_2 | T_{12}(E, I) \mathcal{S}_{12} | \mathbf{p}'_1, \mathbf{p}'_2 \rangle \langle \mathbf{p}'_1, \mathbf{p}'_2 | T_{12}(E, -I) | \mathbf{p}_1, \mathbf{p}_2 \rangle \end{aligned} \quad (3.5)$$

and the loss part is

$$(\mathbf{p}^2; \mathbf{p}^2 | \mathcal{G}_E^{(2)}(I) | \mathbf{p}^2; \mathbf{p}^2) = 2! \langle \mathbf{p}_1, \mathbf{p}_2 | [T_{12}(E, I) - T_{12}(E, -I)] \mathcal{S}_{12} | \mathbf{p}_1, \mathbf{p}_2 \rangle \quad (3.6)$$

By using the identity

$$\prod_{i=1}^n A_i - \prod_{j=1}^n A'_j = \sum_{k=1}^n \sum_{i=1}^{k-1} \prod_{j=k+1}^{n+1} A_i (A_k - A'_k) A'_j, \quad \text{for } A_0 = A'_{n+1} = 1 \quad (3.7)$$

we can rewrite the loss part as

$$\begin{aligned} & (\mathbf{p}^2; \mathbf{p}^2 | \mathcal{G}_E^{(2)}(I) | \mathbf{p}^2; \mathbf{p}^2) \\ &= 2! \sum_{\mathbf{p}_1} \sum_{\mathbf{p}_2} \langle \mathbf{p}_1, \mathbf{p}_2 | T_{12}(E, I) \mathcal{S}_{12} | \mathbf{p}'_1, \mathbf{p}'_2 \rangle \\ & \quad \times \langle \mathbf{p}'_1, \mathbf{p}'_2 | T_{12}(E, -I) | \mathbf{p}_1, \mathbf{p}_2 \rangle \left( \frac{1}{E_{\mathbf{p}^2} - E - (I/2)} - \frac{1}{E_{\mathbf{p}^2} - E + (I/2)} \right) \end{aligned} \quad (3.8)$$

where the symmetrization operator  $\mathcal{S}_{12}$  has been moved into the left  $T$ -matrix.

The calculation with the identity (3.7) can be performed by using the diagrammatic method in a way similar to the method based on the compensative relation discussed in Section 3 of I. That is, to reformulate the loss part,



Fig. 14. Two-particle one-sided skeleton fragment.

$$\chi_E^{(2)} = 2! \left( (i \rightarrow i^<) * \left( \text{diagram} \right) + \left( \text{diagram} \right) \right)$$

Fig. 15. Two-particle collision s. operator.

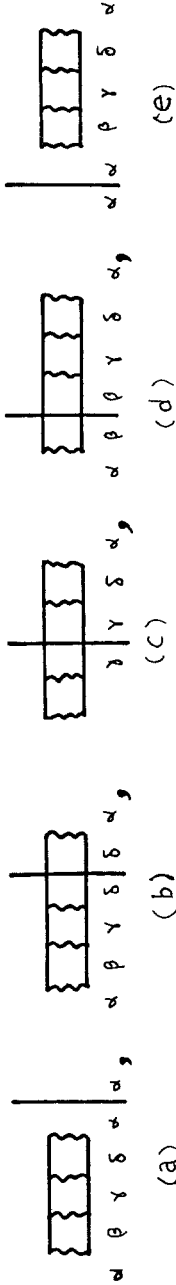


Fig. 16. Examples of diagrams corresponding to the terms in the identity (3.7).

$$3! \left( \left( \text{diagram} \right) + \sum_{P(123)} \left( \text{diagram} \right) + \sum_{P(123)} \left( \text{diagram} \right) \right)$$

Fig. 17. Three-particle one-sided skeleton fragments.

we first draw a one-sided diagonal fragment, such as the example in Fig. 16a. Next, the innermost potential is transferred to the opposite innermost side [diagram (b)]. The third diagram (c) is obtained from the second by a similar transfer of the innermost potential on the left side of the  $\Lambda$  line. The successive transfers are continued until we obtain diagram (e) on the opposite side of the original one. Then, the first and the last diagrams (a) and (e) correspond to the expression in (3.6), while the intermediate diagrams (b)–(d) correspond to (3.8). This diagrammatic relation holds for any diagrams of the loss part, including an arbitrary number of colliding particles.

It is worthwhile noting that if we are interested in the asymptotic kinetic equation, the integration over  $E$  can be performed for the simplest case of  $ct = \text{finite}$  in the limit  $t \rightarrow \infty$ , and the equation for  $\phi_1(\mathbf{p}_1, t)$  can be obtained: Namely, as has been discussed in I, the asymptotic kinetic equation is given by

$$\begin{aligned} i\hbar \partial_t \phi_{1,E}(\mathbf{p}_1, t) &= \frac{2\pi}{\hbar} \int_0^\infty d\tau \sum_{r=2} (h^3 c)^{r-1} \sum_{\mathbf{p}^{r-1}} \sum_{\mathbf{p}^{r'}} (\mathbf{p}^r; \mathbf{p}^r | \chi_E^{(r)}(\tau) | \mathbf{p}^{r'}; \mathbf{p}^{r'}) \\ &\quad \times \prod_{i=0}^r \phi_{1,E}(\mathbf{p}_i, t - \tau) \end{aligned} \quad (3.9)$$

and this is a direct result from the solution for  $\rho_{0,E}(|\mathbf{p}^N; t\rangle)$ ,

$$\begin{aligned} \rho_{0,E}(|\mathbf{p}^N; t\rangle) &= \frac{1}{2\pi i} \sum_{\mathbf{p}^N} \sum_{m=0}^\infty \frac{1}{m!} \left( \frac{-it}{\hbar} + \partial_t \right)^m (\mathbf{p}^N; \mathbf{p}^N | [\chi_E^m(l) \Delta_E(l) \text{ or } \Delta_E(l) \tilde{\chi}_E^m(l)] \\ &= |\mathbf{p}^N; \mathbf{p}^N\rangle \rho_0(|\mathbf{p}^N; 0\rangle) |_{l=+i0} \end{aligned} \quad (3.10)$$

where the destruction part has been omitted for simplicity (see Appendix B in I). In the simplest case with only two-particle collision, the differential term with respect to  $l$  in (3.10) can be neglected. This implies that the contribution of a collision which started at some previous time on the right-hand side of (3.9) can be neglected, i.e.,

$$\begin{aligned} i\hbar [\partial_t \phi_{1,E}(\mathbf{p}_1, t)]^{(2)} &= \frac{2\pi}{\hbar} \int_0^\infty d\tau h^3 c \sum_{\mathbf{p}_2} \sum_{\mathbf{p}_1'} \sum_{\mathbf{p}_2'} (\mathbf{p}^2; \mathbf{p}^2 | \chi_E^{(2)}(\tau) | \mathbf{p}^{2'}; \mathbf{p}^{2'}) \phi_{1,E}(\mathbf{p}_1', t) \phi_{1,E}(\mathbf{p}_2', t) \\ &= h^3 c \sum_{\mathbf{p}_2} \sum_{\mathbf{p}_1'} \sum_{\mathbf{p}_2'} (\mathbf{p}^2; \mathbf{p}^2 | \chi_E^{(2)}(+i0) | \mathbf{p}^{2'}; \mathbf{p}^{2'}) \phi_{1,E}(\mathbf{p}_1', t) \phi_{1,E}(\mathbf{p}_2', t) \end{aligned} \quad (3.11)$$

$$\begin{aligned}
 & 3! (i^2 + i^4) * \left\{ \begin{array}{l} \text{Diagram 1} \\ \text{Diagram 2} \\ \text{Diagram 3} \end{array} \right\} + \sum_{P(123)} \left( \begin{array}{l} \text{Diagram 4} \\ \text{Diagram 5} \\ \text{Diagram 6} \end{array} \right) + \left( \begin{array}{l} \text{Diagram 7} \\ \text{Diagram 8} \\ \text{Diagram 9} \end{array} \right) \\
 & + \sum_{P(123)} \left( \begin{array}{l} \text{Diagram 10} \\ \text{Diagram 11} \\ \text{Diagram 12} \end{array} \right) + \left( \begin{array}{l} \text{Diagram 13} \\ \text{Diagram 14} \\ \text{Diagram 15} \end{array} \right) \\
 & + \sum_{P(123)} \left( \begin{array}{l} \text{Diagram 16} \\ \text{Diagram 17} \\ \text{Diagram 18} \end{array} \right) + \left( \begin{array}{l} \text{Diagram 19} \\ \text{Diagram 20} \\ \text{Diagram 21} \end{array} \right)
 \end{aligned}$$

The diagrams are Feynman-like diagrams for three-particle interactions. They consist of circles representing particles, with lines connecting them. Some circles are labeled with '2' or '3'. Some lines are labeled with '1', '2', '3' or 'a', 'b'. Some diagrams have superscripts like (3) or subscripts like s, b. The diagrams are arranged in three rows, each representing a different part of the equation. The first row shows a sum of three diagrams in curly braces, followed by a sum over permutations P(123) of three diagrams, and then three more diagrams. The second row shows a sum over permutations P(123) of three diagrams, followed by three more diagrams. The third row shows a sum over permutations P(123) of three diagrams, followed by three more diagrams.

Fig. 18. Three-particle two-sided skeleton fragments.



For such a case, we have

$$\rho_{0^+ E}(|\mathbf{p}^N; t) = \delta(E - E_{\mathbf{p}^N})\rho_0(|\mathbf{p}^N; t) \quad (3.12)$$

from (3.10). Then, substituting (3.12), (3.5), and (3.8) into (3.11), and integrating over  $E$ , we find the asymptotic kinetic equation,

$$\begin{aligned} & [\partial_t \phi_1(\mathbf{p}_1, t)]^{(2)} \\ &= 2! \frac{2\pi\hbar^3 c}{\hbar} \sum_{\mathbf{p}_2} \sum_{\mathbf{p}_1'} \sum_{\mathbf{p}_2'} \langle \mathbf{p}_1, \mathbf{p}_2 | T_{12}(E_{\mathbf{p}_1, \mathbf{p}_2}) \mathcal{S}_{12} | \mathbf{p}_1', \mathbf{p}_2' \rangle \\ & \quad \times \langle \mathbf{p}_1', \mathbf{p}_2' | T_{12}^\dagger(E_{\mathbf{p}_1, \mathbf{p}_2}) | \mathbf{p}_1, \mathbf{p}_2 \rangle \delta(E_{\mathbf{p}_1} + E_{\mathbf{p}_2} - E_{\mathbf{p}_1'} - E_{\mathbf{p}_2'}) \\ & \quad \times [\phi_1(\mathbf{p}_1', t)\phi_1(\mathbf{p}_2', t) - \phi_1(\mathbf{p}_1, t)\phi_1(\mathbf{p}_2, t)] \end{aligned} \quad (3.13)$$

where the argument  $+i0$  in the  $T$ -matrix is omitted for simplicity and the dagger ( $\dagger$ ) means the Hermite conjugate of the operator.

As a second example we consider three-particle collisions. The basic unsymmetrized clusters were already shown in Fig. 5. Following the rule for symmetrization given in the previous section, we get the quantum statistical one-sided skeleton fragments shown in Fig. 17, where  $\mathcal{S}_b^{(3)}$  and  $\mathcal{S}_{sb}^{(3)}$  are partial symmetrization operators for diagrams having a bubble and a semibubble, and are defined by

$$3! \mathcal{S}_b^{(3)} = 3! \mathcal{S}_{123} - 2! \mathcal{S}_{23}, \quad 3! \mathcal{S}_{sb}^{(3)} = 3! \mathcal{S}_{123} - 2! \theta Q_{12} \mathcal{S}_{23} \quad (3.14)$$

Then, by using the compensative relation, we obtain the two-sided skeleton fragments shown in Fig. 18. For the three-particle collision, we have in addition diagonal fragments having a bubble, or an inactivated diagonal fragment, or an external contraction. Such one-sided and two-sided fragments are shown in Figs. 19a and 19b, respectively.

The corresponding expression can be written down explicitly by using the two-particle  $T$ -matrix (3.3) and the three-particle  $T$ -matrix defined by

$$T^{(3)}(E, l) = \sum_{i < j}^3 V_{ij} - \sum_{i < j}^3 V_{ij} \frac{1}{H_{123}^0 - E - (l/2)} T^{(3)}(E, l) \quad (3.15)$$

where  $H_{123}^0$  is the three-particle unperturbed Hamiltonian.

We give here the kinetic equation for the interesting situation in which the collision time  $t_c$  can be regarded as being instantaneous as compared with the relaxation time  $t_r$ . For such a system, not only the terms differentiated with respect to  $l$ , but also the terms having bubbles or inactivated diagonal fragments can be neglected in (3.10). This implies that (3.12) again holds. Then, writing down the expression corresponding to the diagrams in Figs. 17–19 and reformulating the loss part with the identity (3.7) by the aid of the diagrammatic

$$\begin{aligned}
 \text{(a)} \quad & \sum_{P(123)} \left\{ (2!)^2 \left( \begin{array}{c} \text{---} \textcircled{2} \textcircled{2} \textcircled{2} \text{---} \\ \text{---} \textcircled{2} \textcircled{2} \textcircled{2} \text{---} \\ \text{---} \textcircled{2} \textcircled{2} \textcircled{2} \text{---} \end{array} \right) + 2! \left( \begin{array}{c} \text{---} \textcircled{2} \textcircled{2} \textcircled{2} \text{---} \\ \text{---} \textcircled{2} \textcircled{2} \textcircled{2} \text{---} \\ \text{---} \textcircled{2} \textcircled{2} \textcircled{2} \text{---} \end{array} \right) \right\} \\
 \text{(b)} \quad & (2!)^2 \sum_{P(123)} \left\{ (i^> + i^<) * \left( \begin{array}{c} \text{---} \textcircled{2} \textcircled{2} \textcircled{2} \text{---} \\ \text{---} \textcircled{2} \textcircled{2} \textcircled{2} \text{---} \\ \text{---} \textcircled{2} \textcircled{2} \textcircled{2} \text{---} \end{array} \right) + \left( \begin{array}{c} \text{---} \textcircled{2} \textcircled{2} \textcircled{2} \text{---} \\ \text{---} \textcircled{2} \textcircled{2} \textcircled{2} \text{---} \\ \text{---} \textcircled{2} \textcircled{2} \textcircled{2} \text{---} \end{array} \right) * \left( \begin{array}{c} \text{---} \textcircled{2} \textcircled{2} \textcircled{2} \text{---} \\ \text{---} \textcircled{2} \textcircled{2} \textcircled{2} \text{---} \\ \text{---} \textcircled{2} \textcircled{2} \textcircled{2} \text{---} \end{array} \right) \right\} \\
 & + 2! \sum_{P(123)} \left( \begin{array}{c} \text{---} \textcircled{2} \textcircled{2} \textcircled{2} \text{---} \\ \text{---} \textcircled{2} \textcircled{2} \textcircled{2} \text{---} \\ \text{---} \textcircled{2} \textcircled{2} \textcircled{2} \text{---} \end{array} \right) + \left( \begin{array}{c} \text{---} \textcircled{2} \textcircled{2} \textcircled{2} \text{---} \\ \text{---} \textcircled{2} \textcircled{2} \textcircled{2} \text{---} \\ \text{---} \textcircled{2} \textcircled{2} \textcircled{2} \text{---} \end{array} \right) + \left( \begin{array}{c} \text{---} \textcircled{2} \textcircled{2} \textcircled{2} \text{---} \\ \text{---} \textcircled{2} \textcircled{2} \textcircled{2} \text{---} \\ \text{---} \textcircled{2} \textcircled{2} \textcircled{2} \text{---} \end{array} \right)
 \end{aligned}$$

Fig. 19. Three-particle diagonal fragments having a bubble, or an inactivated diagonal fragment, or an external contraction.

method, and further moving the symmetrization operators into the left-hand  $T$ -matrices, we get the contribution of the three-particle collisions

$$\begin{aligned}
 & [\partial_t \phi_1(\mathbf{p}_1, t)]^{(3)} \\
 &= 3! \frac{2\pi(h^3 c)^2}{\hbar} \sum_{\mathbf{p}_2} \sum_{\mathbf{p}_3} \sum_{\mathbf{p}_1'} \sum_{\mathbf{p}_2'} \sum_{\mathbf{p}_3'} \{ \langle \mathbf{p}_1, \mathbf{p}_2, \mathbf{p}_3 | T_{ir}^{(3)} \mathcal{S}_{123} | \mathbf{p}_1', \mathbf{p}_2', \mathbf{p}_3' \rangle \\
 & \quad \times \langle \mathbf{p}_1', \mathbf{p}_2', \mathbf{p}_3' | T_{ir}^{(3)\dagger} | \mathbf{p}_1, \mathbf{p}_2, \mathbf{p}_3 \rangle \\
 & \quad + \sum_{P(123)} [ \langle \mathbf{p}_1, \mathbf{p}_2, \mathbf{p}_3 | T_{23} \mathcal{S}_{123} | \mathbf{p}_1', \mathbf{p}_2', \mathbf{p}_3' \rangle \\
 & \quad \times \langle \mathbf{p}_1', \mathbf{p}_2', \mathbf{p}_3' | T_{ir}^{(3)\dagger} | \mathbf{p}_1, \mathbf{p}_2, \mathbf{p}_3 \rangle + \text{c.c.} ] \\
 & \quad + \sum_{P(123)} \langle \mathbf{p}_1, \mathbf{p}_2, \mathbf{p}_3 | T_{12} R_0^{(3)} (T_{23} \mathcal{S}_b^{(3)} + T_{13} \mathcal{S}_{sb}^{(3)}) | \mathbf{p}_1', \mathbf{p}_2', \mathbf{p}_3' \rangle \\
 & \quad \times \langle \mathbf{p}_1', \mathbf{p}_2', \mathbf{p}_3' | T_{23}^\dagger R_0^{(3)\dagger} T_{12}^\dagger | \mathbf{p}_1, \mathbf{p}_2, \mathbf{p}_3 \rangle \\
 & \quad - \sum_{P(123)} [ \langle \mathbf{p}_1, \mathbf{p}_2, \mathbf{p}_3 | (1 - T_{23} R_0^{(3)}) T_{12} R_0^{(3)} (T_{23} \mathcal{S}_b^{(3)} \\
 & \quad + T_{13} \mathcal{S}_{sb}^{(3)}) | \mathbf{p}_1', \mathbf{p}_2', \mathbf{p}_3' \rangle \langle \mathbf{p}_1', \mathbf{p}_2', \mathbf{p}_3' | T_{23}^\dagger | \mathbf{p}_1, \mathbf{p}_2, \mathbf{p}_3 \rangle + \text{c.c.} ] \\
 & \quad \times \delta(E_{\mathbf{p}_1} + E_{\mathbf{p}_2} + E_{\mathbf{p}_3} - E_{\mathbf{p}_1'} - E_{\mathbf{p}_2'} - E_{\mathbf{p}_3'}) \\
 & \quad \times [\phi_1(\mathbf{p}_1', t) \phi_1(\mathbf{p}_2', t) \phi_1(\mathbf{p}_3', t) - \phi_1(\mathbf{p}_1, t) \phi_1(\mathbf{p}_2, t) \phi_1(\mathbf{p}_3, t)] \\
 & \quad + 2! \frac{2\pi h^3 c}{\hbar} \sum_{\mathbf{p}_2} \sum_{\mathbf{p}_1'} \sum_{\mathbf{p}_2'} \{ \langle \mathbf{p}_1, \mathbf{p}_2 | T_{12} \mathcal{S}_{12} | \mathbf{p}_1', \mathbf{p}_2' \rangle \langle \mathbf{p}_1', \mathbf{p}_2' | T_{12}^\dagger | \mathbf{p}_1, \mathbf{p}_2 \rangle \\
 & \quad \times \delta(E_{\mathbf{p}_1} + E_{\mathbf{p}_2} - E_{\mathbf{p}_1'} - E_{\mathbf{p}_2'}) \{ \phi_1(\mathbf{p}_1', t) \phi_1(\mathbf{p}_2', t) \theta h^3 c [\phi_1(\mathbf{p}_1, t) \\
 & \quad + \phi_1(\mathbf{p}_2, t)] - \phi_1(\mathbf{p}_1, t) \phi_1(\mathbf{p}_2, t) \theta h^3 c [\phi_1(\mathbf{p}_1', t) + \phi_1(\mathbf{p}_2', t)] \} \\
 & \quad - \sum_{\mathbf{p}_1'} \sum_{\mathbf{p}_2'} \{ \langle \mathbf{p}_1, \mathbf{p}_2 | T_{12} | \mathbf{p}_1'', \mathbf{p}_2'' \rangle \\
 & \quad \times \frac{1}{E_{\mathbf{p}_1'', \mathbf{p}_2''} - E_{\mathbf{p}_1, \mathbf{p}_2} - i0} \theta h^3 c [\phi_1(\mathbf{p}_1'', t) + \phi_1(\mathbf{p}_2'', t)] \\
 & \quad \times \langle \mathbf{p}_1'', \mathbf{p}_2'' | T_{12} \mathcal{S}_{12} | \mathbf{p}_1', \mathbf{p}_2' \rangle \langle \mathbf{p}_1', \mathbf{p}_2' | T_{12}^\dagger | \mathbf{p}_1, \mathbf{p}_2 \rangle + \text{c.c.} \} \\
 & \quad \times \delta(E_{\mathbf{p}_1} + E_{\mathbf{p}_2} - E_{\mathbf{p}_1'} - E_{\mathbf{p}_2'}) [\phi_1(\mathbf{p}_1', t) \phi_1(\mathbf{p}_2', t) \\
 & \quad - \phi_1(\mathbf{p}_1, t) \phi_1(\mathbf{p}_2, t)] \} \tag{3.16}
 \end{aligned}$$

where

$$R_0^{(3)} = 1/(H_{123}^0 - E_{\mathbf{p}_1, \mathbf{p}_2, \mathbf{p}_3} - i0) \tag{3.17}$$

and the abbreviations  $T_{ir}^{(3)} \equiv T_{ir}^{(3)}(E_{\mathbf{p}_1, \mathbf{p}_2, \mathbf{p}_3} + i0)$  and  $T_{ij} \equiv T_{ij}(E_{\mathbf{p}_i, \mathbf{p}_j} + i0)$  have been used.

#### 4. DISCUSSION

Expression (3.16) shows that the symmetrized collision terms containing three particles are classified into two groups: One group is made up of the first part of (3.16), corresponding to Figs. 17 and 18, and describes essentially three-particle collisions. We have succeeded in the symmetrization of this type of interaction through our contracting procedure on the basis of the unsymmetrized three-particle collision *s*-operator. The other group is made up of the second part of (3.16), corresponding to Fig. 19, and describes the symmetry effect on the initial and final states in the two-particle collision, i.e., the Uehling-Uhlenbeck term (the first term in this part), and on the intermediate states in this collision (the second term in this part), which was first derived by Prigogine and Résibois.<sup>(4)</sup> These terms have been obtained merely by putting an external contraction on the two-particle collision *s*-operator.

The order of magnitude of these terms has been discussed for the unsymmetrized three-particle collision by Résibois<sup>(2)</sup> and for the intermediate statistical effect by Prigogine and Résibois.<sup>(4)</sup> For the case of  $\lambda_B \gg a$  (where  $\lambda_B$  is the de Broglie wavelength and  $a$  is the molecular length), their estimations still hold for our symmetrized terms, since for such a case the exchange collision may give a contribution of the same order as the direct collision. Thus, following their estimation, we have

$$\frac{P_{III,III}}{P_{II,II}} \sim \frac{\lambda_B}{a} a^3 c, \quad \frac{P_{II,III}}{P_{II,II}} \sim \frac{a}{\lambda_B} \lambda_B^3 c \quad (4.1)$$

for the first part of (3.16), and

$$\frac{P_{II,U}}{P_{II,II}} \sim \lambda_B^3 c, \quad \frac{P_{II,E}}{P_{II,II}} \sim \frac{a}{\lambda_B} \lambda_B^3 c \quad (4.2)$$

for the second part of (3.16). Here,  $P_{II,II}$  is a typical magnitude of the contribution from the two-particle collision in (3.13),  $P_{III,III}$  is that from the three-particle collision in which three particles appear on both sides of the  $\Lambda$  line, as in the first diagram in Fig. 18, and  $P_{II,III}$  is that in which two and three particles appear on each side of the  $\Lambda$  line, respectively, as in the second diagram in Fig. 18. Further,  $P_{II,U}$  is the contribution from the Uehling-Uhlenbeck term, as in the second diagram with external contraction in Fig. 19b, and  $P_{II,E}$  is that from the two-particle collision with external contraction in the intermediate state, as in the last diagram in Fig. 19b. Thus, for the case

$$\lambda_B < a < c^{-1/3} \quad (4.3)$$

the real three-particle collision is the most important, the terms  $P_{II,III}$  and  $P_{II,E}$  give the first correction terms, and the Uehling-Uhlenbeck term is the smallest one. In contrast, for the case

$$a < c^{-1/3} < \lambda_B \quad (4.4)$$

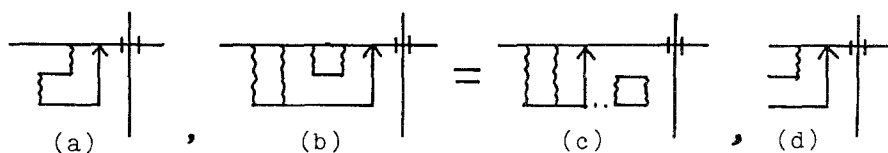


Fig. 20. Diagrams containing the same pattern of an interaction.

the situation is reversed, namely, the dominant term is now the Uehling-Uhlenbeck term and the smallest term is  $P_{\text{III,III}}$ .

Finally, we mention why we have symmetrized the collision operator on the basis of the cluster expansion rather than by constructing effective vertices by incorporating the quantum statistical effect into a single potential such as in our previous work<sup>(15)</sup> or in Balescu's work.<sup>(6)</sup> The reason is most easily seen by using the diagrams in Fig. 20, where diagrams (a) and (b) contain the same pattern of the interaction (d). However, it is more natural to incorporate the effect of the symmetrization in (b) into the outside interaction as in (c). This shows that this type of contraction cannot be classified into a single pattern. Hence, it is more appropriate to classify the effect of the symmetrization on the basis of the cluster expansion. Furthermore, it must be remarked that our method based on this idea seems to be closely related to the quantum statistical equilibrium theory given by Lee and Yang.<sup>(1)</sup> A detailed study of this relationship will be presented separately.

## ACKNOWLEDGMENTS

We thank Prof. N. Mishima for stimulating interest in this work and for many fruitful discussions. We express our gratitude to Prof. R. Suzuki for his hospitality and for valuable discussions.

## REFERENCES

1. N. Mishima, T. Petrosky, and R. Suzuki, *J. Stat. Phys.*, this issue, preceding paper.
2. P. Résibois, *Physica* **27**:33 (1961); **31**:645 (1965).
3. R. Swenson, *J. Math. Phys.* **4**:544 (1963).
4. I. Prigogine and P. Résibois, *Physica* **24**:795 (1958).
5. N. Mishima, T. Petrosky, and M. Yamazaki, *J. Stat. Phys.* **14**:359 (1976).
6. R. Balescu, *Physica* **62**:485 (1972).
7. T. Lee and C. Yang, *Phys. Rev.* **113**:1165 (1959); **116**:25 (1959); **117**:12 (1960); **117**:22 (1960).